

GROUND-TRUTHING SEISMIC REFRACTION TOMOGRAPHY FOR SINKHOLE DETECTION IN FLORIDA

Dennis R. Hiltunen¹, Nick Hudyma², Timothy P. Quigley³, and Chandra Samakur⁴

¹University of Florida, Gainesville, FL, USA; dhilt@ce.ufl.edu

²University of North Florida, Jacksonville, FL, USA; nhudyma@unf.edu

³University of Florida, Gainesville, FL, USA; tquigley@ufl.edu

⁴Florida Department of Transportation, Lake City, FL, USA; chandra.samakur@dot.state.fl.us

ABSTRACT

During a recent ground proving exercise at the University of North Florida/University of Florida karstic limestone geophysical/ground proving test site in central Florida, the limestone bedrock surface was mapped along several survey lines using both intrusive and geophysical techniques. Analyses of site data revealed a highly erratic limestone bedrock surface, which is common in karst terrane. Analysis of seismic refraction data demonstrated that the refraction tomography software system was able to reveal the undulating bedrock surface. However, the tomography data revealed marked differences in the compression wave velocities at the top of the bedrock surface at various locations along one of the survey lines. Compression wave velocities were highest within slots or valleys and lowest at the tops of blocks or pinnacles. Ground proving via cone penetration tests and geotechnical borings appears to corroborate this finding, and demonstrates the importance of measuring multiple material parameters during site characterization activities in complex terrane. Finally, two sinkholes formed in the detention pond directly over two valley/bowl features after refraction testing was completed, demonstrating that refraction tomography has potential in identifying areas at risk for sinkhole development.

INTRODUCTION

In order to provide effective return of storm water runoff to the subsurface aquifer, the Florida Department of Transportation (FDOT) constructs detention basins adjacent to its transportation facilities. These basins serve as a collection point for runoff within a local drainage area, and the overburden soil above the aquifer provides a natural filter for contaminants in the surface runoff water. However, the geologic setting for many of these basins in Florida is karst, limestone bedrock at shallow depth, and the concentration of water flow in these basins leads to frequent development of sinkholes. These sinkholes are an environmental hazard, as they provide a direct, open conduit for contaminant-laden runoff water to return to the aquifer rather than percolate through the overburden soil. Consequently, FDOT is keenly interested in all aspects of sinkholes, including factors leading to formation, methods of early detection, and effective methods for rapid repair.

Recently, FDOT has engaged in a research effort to evaluate the capabilities of a wide range of geophysical investigation tools with regard to detection of sinkhole-prone areas within sites being considered for construction of detention ponds. The geophysical techniques evaluated have included ground penetrating radar (GPR), multi-electrode electrical resistivity (MER), seismic MASW, and seismic refraction tomography. In addition to geophysical testing at the research sites, extensive traditional geotechnical site characterization has been conducted, including boring and sampling of soil and rock, standard penetration tests (SPT), and cone penetration tests (CPT).

The paper will evaluate the capabilities of seismic refraction tomography (Carpenter, et al., 2003; Cramer and Hiltunen, 2004; Hiltunen and Cramer, 2006; and Sheehan, *et al.*, 2005). Comparisons between refraction tomograms and borehole logs, SPT soundings, and CPT soundings suggest that the refraction method can map the laterally-variable top of bedrock surface typical of karst terrane.

GEOPHYSICAL/GROUND PROVING TEST SITE

Location

The University of North Florida (UNF) and the University of Florida (UF) have developed a Florida Department of Transportation (FDOT) dry retention pond into a karstic limestone geophysical/ ground proving test site in Alachua County, Florida. The site contains a number of survey lines and 5 PVC-cased boreholes extending to approximately 15 meters. The test site is unique because the northern portion of the retention pond commonly experiences sinkhole activity, whereas the southern portion rarely experiences sinkhole activity.

The geophysical/ground proving test site is located outside of Newberry, Florida on State Road 26 in Alachua County. The site is approximately 29 kilometers from Gainesville, and approximately 150 kilometers from Jacksonville. The location of the test site within the state and Alachua County is shown in figure 1a. The test site is a dry retention pond, approximately 1.6 hectares in size. The northern portion of the site has been susceptible to sinkhole formation and a number of large sinkholes have formed and been repaired. However, the southern portion has been relatively free of sinkholes and is an ideal location for characterizing karst limestone sites. The two zones within the test site are shown in figure 1b.

Shallow Subsurface Stratigraphy

In Alachua County, the overburden material is undifferentiated, siliciclastic sediments that overlie the Hawthorn Group that overlie the Ocala Limestone. The undifferentiated, siliciclastic sediments are late Miocene to Plio-Pliocene in age. The dominant lithology is quartz sands that contain variable mixtures of clay. The sands range from fine to very coarse, and may include some gravel-sized particles. The sediments range in color from white to reddish orange. This unit virtually blankets Alachua County ranging in depth from a few meters to greater than 6 m thick (Campbell and Scott, 1991).

The age of the Hawthorn Group is Miocene to early Plio-Pliocene. The Hawthorn Group consists of interbedded and intermixed carbonate and siliciclastics containing varying percentages of phosphate grains. The Hawthorn Group has variable thickness within the region and lies unconformably on the Ocala Limestone. Where the Hawthorn Group is not present, the undifferentiated siliciclastic sediments lie unconformably on the Ocala Limestone (Scott, 2001 and Campbell and Scott, 1991).

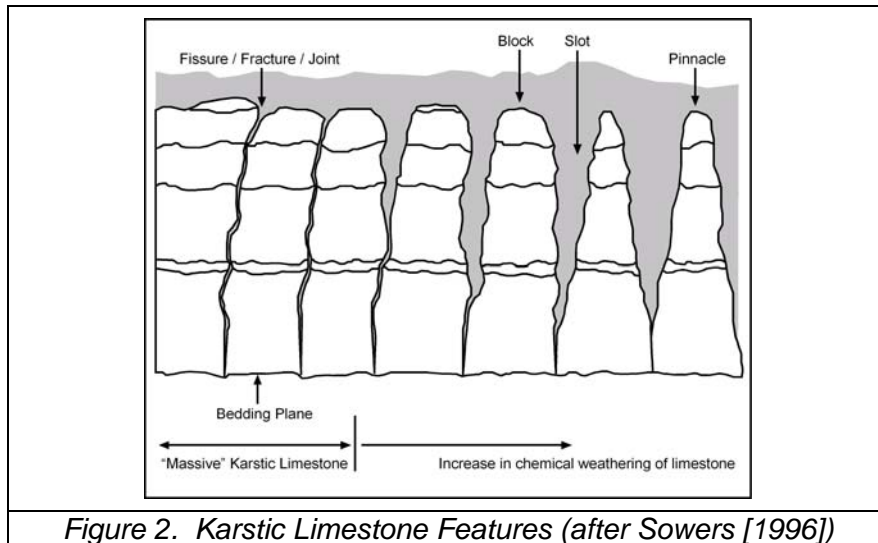
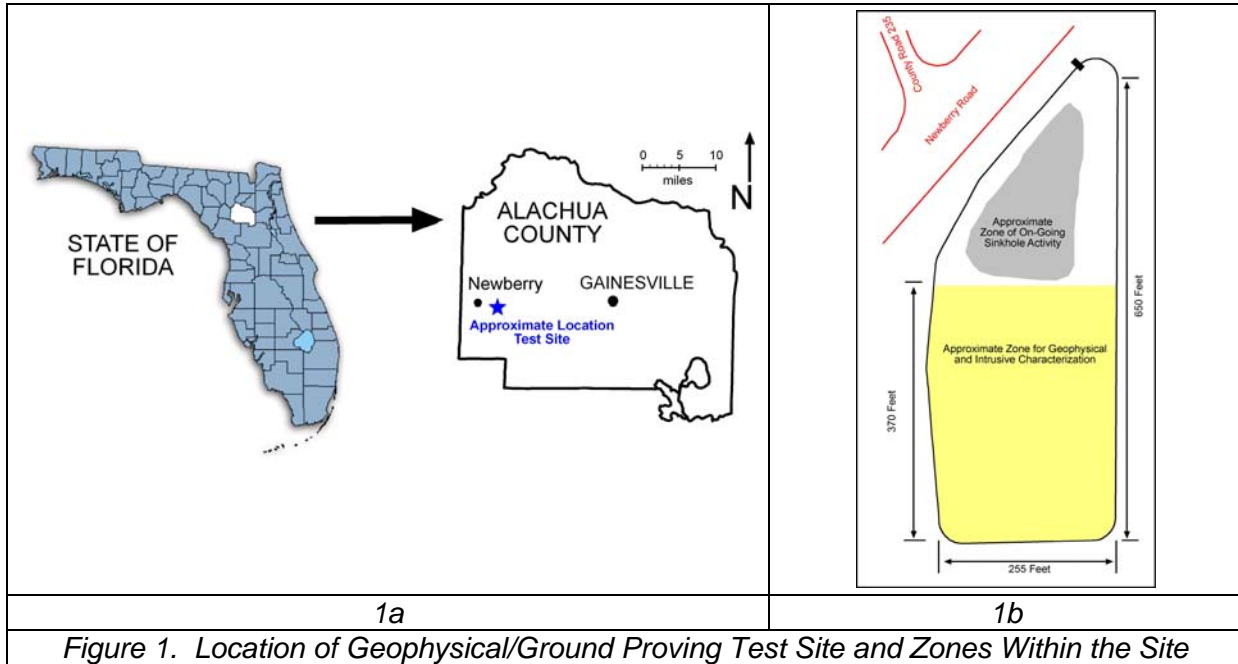
Underlying the Hawthorn Group or the undifferentiated, siliciclastic sediments is the Ocala Limestone, which is Upper Eocene in age. It consists of nearly pure limestone and dolostones (Scott, 2001). The top of the limestone is extremely variable due to karstification and erosion.

Features in Karstic Limestone

Karst is a type of topography formed in unconsolidated sediments (soils) that overlie limestone, dolomite, or other soluble rock. The surface of the soluble rock may be erratic and highly variable indicating that chemical dissolution/weathering is presently occurring or had occurred before the soil was deposited, or the surface may be relatively flat indicating that chemical dissolution/weathering has not extensively occurred. The term "karstic limestone" is used to describe a limestone lithology that has undergone chemical weathering.

The features associated with karstic limestone are shown in figure 2. Karstic limestone, in what can be considered its massive state, consists of bedding planes and fissures/fractures/ joints. The bedding planes represent the various depositional events that formed the limestone. These features are roughly horizontal and their spacing depends upon the duration of each depositional event and the amount of weathering that occurred during deposition. There are also roughly vertical features within the limestone, which can be described as fissures, fractures, or joints, depending upon their geologic formation.

Over time, chemical weathering occurs within the limestone and the vertical discontinuities become enlarged and form slots. Slots may remain narrow or they may enlarge to form “valleys” or “bowls”. As the limestone weathers, it transitions from a massive structure through the block structures to pinnacles, which is depicted from left to right in figure 2.



SEISMIC REFRACTION TOMOGRAPHY

Field Testing

The southern portion of the test site was subdivided into 26 north-south survey lines equally spaced a distance of 3.0 m (10 ft) apart. The lines were labeled A through Z from west to east across the site, and each line was 85.3 m (280 ft) long, with station 0 m located at the southern end of the site. Two 36.6-m (120-ft) long refraction surveys were conducted during summer 2005 end-to-end along lettered site lines A, F, K, P, U, and Z, and beginning at station 0. Thus, the 12 refraction lines surveyed six of the site lines from station 0 to 73.2 m (240 ft).

Each 36.6-m (120-ft) long refraction survey was conducted with 4.5 Hz vertical geophones spaced equally at 0.61 m (2 ft). Seismic energy was created by vertically striking a metal ground plate with an 89 N (20 lb) sledgehammer, thus producing compression wave (P-wave) first arrivals. Shot locations were spaced at 3.0-m (10-ft) intervals along the 36.6-m (120-ft) line and starting at 0 m, for a total of 13 shots. A 32-channel dynamic signal analyzer was used to collect time records, thus each line was conducted in two stages, i.e., 0-18.3 (0-60) and 18.3-36.6 m (60-120 ft), with each of the 13 shot locations visited twice for each 36.6-m (120-ft) survey.

Travel time records were transferred to the PickWin program (a module of the Seisimager refraction system described below), where geophone and shot geometry were implanted with the records, and first arrivals were determined and saved for analysis with three tomography programs. By way of example, first-arrival travel time curves for the two end-to-end surveys along the A line are shown in figures 3a and 4a, respectively. Data for line A was chosen for presentation herein because these refraction results displayed the most variable conditions along the line, and this line consequently received considerable attention during intrusive ground proofing investigations described below.

Seisimager

The commercially-available Seisimager refraction tomography software system was used to produce P-wave velocity tomograms for each of the 12 travel time data sets. The Seisimager system is well described by its authors and in several recent publications by users of this system. The following statements provide a very brief overview, as well as a listing of key references for the reader to locate further details. As with most tomography systems, Seisimager contains three important components: 1) a forward model for calculating source to receiver first arrival times based upon the current velocity model, 2) an inversion routine for adjusting the velocity model until an acceptable match between calculated and measured first-arrival travel times is obtained, and 3) a means for generating an initial velocity model.

Seisimager is based upon a nonlinear travel time tomography methodology described by Hayashi and Takahashi (2001). A shortest-path algorithm described by Moser (1991) constitutes the forward model, and inversion is accomplished via the simultaneous iterative reconstruction technique (SIRT). An initial velocity model can be created in two ways (Sheehan, *et al.*, 2005): 1) by converting the results from a simple time-term inversion algorithm included in the program to a two-dimensional cell model, or 2) by generating a two-dimensional starting model from user input of the expected velocity range, depth to the deepest layer, and the number of layers in which to divide the zone. In either case, the program will generate the geometry and velocity distribution for the initial model.

Tomography Results

The 12 refraction surveys described above were processed by Seisimager, and P-wave velocity tomograms were produced. To improve quality and uniformity, tomograms from the program were exported to the Surfer graphical software, and the data was plotted with a consistent set of spatial and velocity scales. By way of example, figures 3b and 4b present the optimum velocity tomograms for the two end-to-end surveys along the A line (travel time data presented in figures 3a and 4a, respectively).

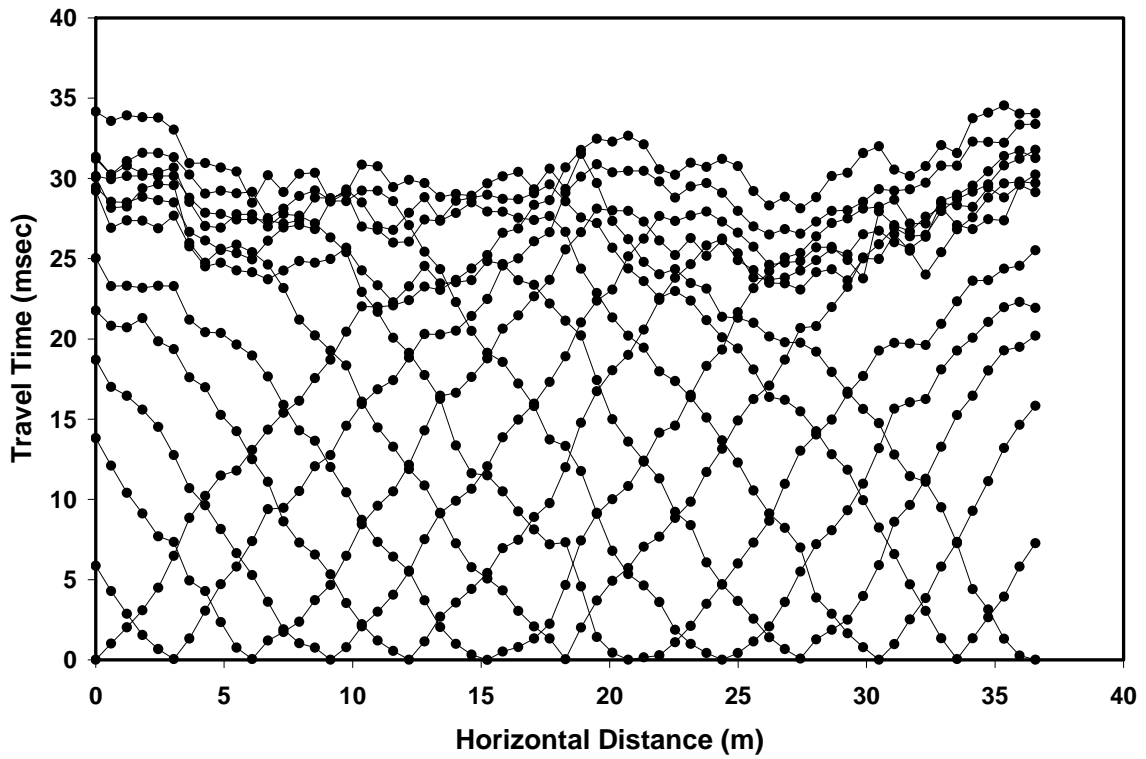


Figure 3a. *Travel Time Curves, A Line, Station 0-36.6 m*

For each set of travel time data, multiple runs of the system were conducted to exercise each model over a wide range of available input parameters. From these multiple runs, a best tomogram was selected based upon several criteria, including: 1) goodness of fit between calculated and measured travel times, 2) distribution of ray path coverage within the model, and 3) number of suspected artifacts within the tomogram. The following observations are offered pertaining to these results:

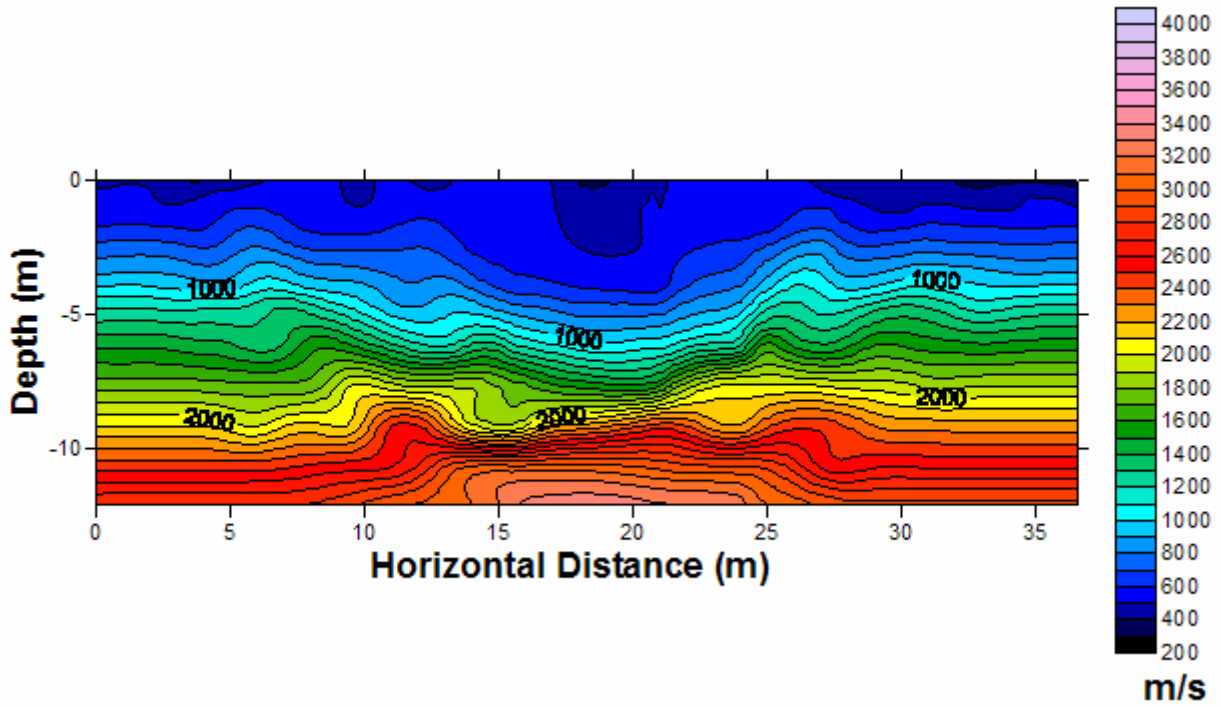


Figure 3b. P-Wave Tomogram, A Line, Station 0-36.6 m

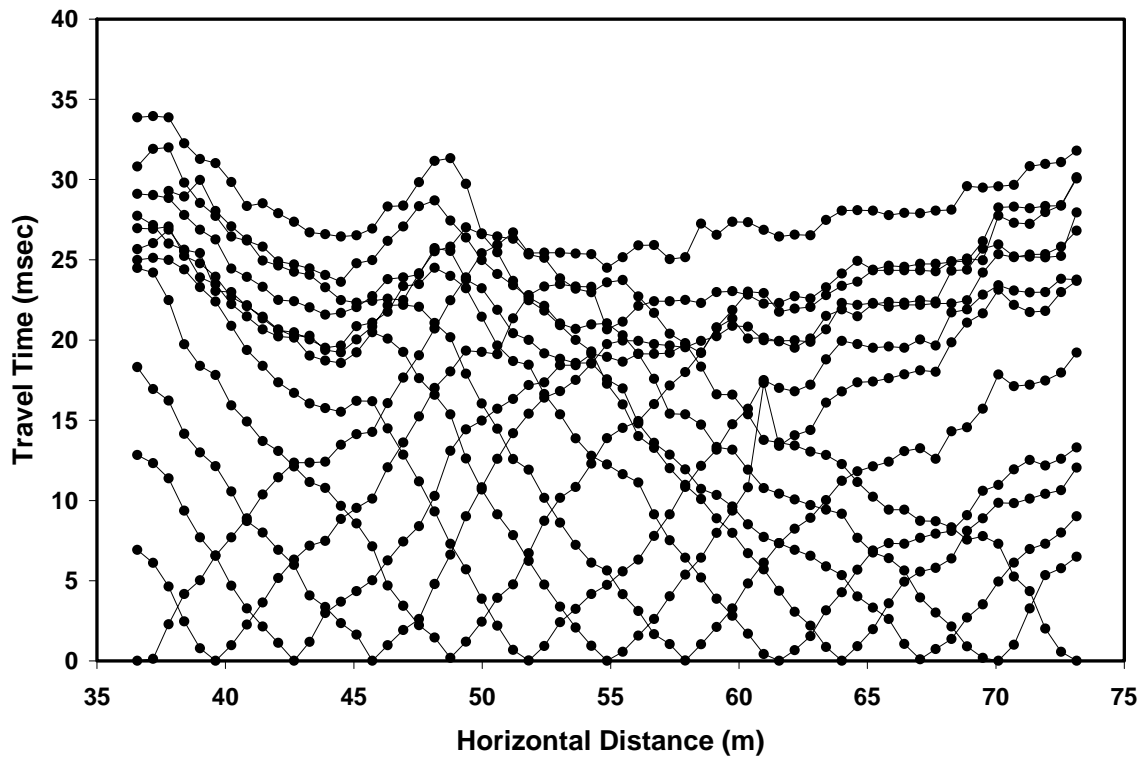


Figure 4a. Travel Time Curves, A Line, Station 36.6-73.2 m

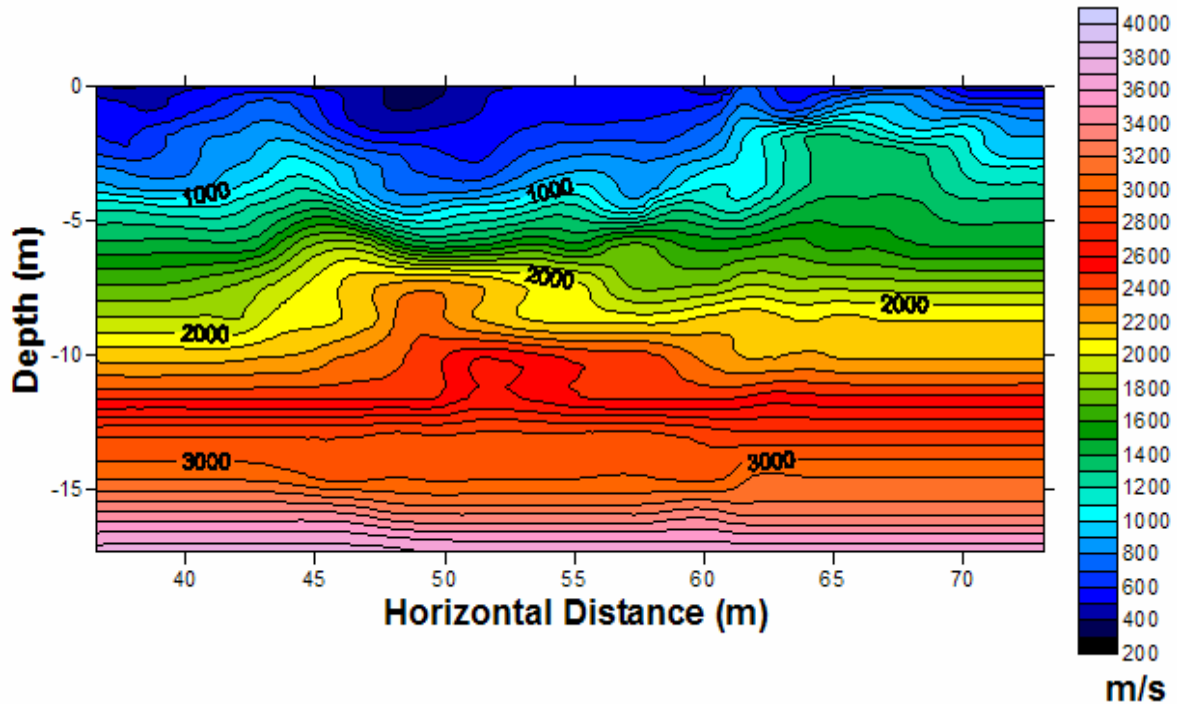


Figure 4b. P-Wave Tomogram, A Line, Station 36.6-73.2 m

- Seisimager produces a tomogram rectangular in shape. In fact, there is little or no ray path coverage near the model edges, and Seisimager extrapolates the interior of the model to produce a rectangular shape. This information should be used with caution.
- It is observed that the gross features of the site profile for the two A lines are similar: there appears to be a valley/bowl near the middle, and blocks/pinnacles near the left and right ends.

The above observations are made herein in regards to the two examples presented. However, it should also be noted that these findings were also observed for the remaining 10 lines. Space limitations obviously prevent presentation of all of this evidence.

GROUND TRUTH

Following refraction data collection and analysis, invasive ground proving information was collected at the site to provide partial verification of the refraction test result interpretations.

Cone Penetration Tests (CPT)

Ten CPT soundings were conducted at strategic locations across the site. The refraction tomograms were used to select these locations, and typically they were chosen to be within a valley or atop a block as described in the previous section. Because line A displayed the most lateral variability along the line, four of the 10 soundings were conducted along line A. These four tests were located at the following horizontal stations: 19.8, 39.6, 44.2, and 65.5 m, and the measured tip resistance results are shown in figure 5. These results are compared with the refraction tomograms from figures 3b and 4b as follows:

- At station 19.8 m, the CPT tip resistance approached a large value of 30 MPa, and the test was terminated at a depth of about 9.2 m. Station 19.8 m is near the middle of a valley feature on the tomograms (figure 3b), and the CPT tip terminates at a P-wave velocity of ± 2000 m/s.

- The sounding at 39.6 m was terminated at shallow depth prematurely because the CPT rod system was bending seriously to the south as penetration was attempted. It is interesting to note on the tomograms (figure 4b) that station 39.6 m is slightly to the left of a block/pinnacle feature, and bending of the CPT rod to the south at the site (to the left or lower station number on tomogram) is consistent with this block feature.
- At stations 44.2 and 65.5 m, the CPT tip resistance approached a large value of 30 MPa, and the tests were terminated at shallow depths less than 0.5 m. Stations 44.2 and 65.5 m are both located near the top of block/pinnacle features on the tomograms (figure 4b). However, in contrast to station 19.8 m, the CPT tips terminated at P-wave velocities less than 1000 m/s at stations 44.2 and 65.5 m.
- It is reported that small, rock outcrops were visible near stations 62.5-64 m and 66.1-67.1 m, which are on both sides of the CPT sounding at 65.5 m.
- Finally, it is reported that similar results as described above were discovered for the remaining six CPT soundings across the site. Three “deep” soundings terminated within valleys/bowls on the tomograms. Three “shallow” soundings terminated near the top of block/pinnacle features on the tomograms at relatively lower P-wave velocities as compared to the “deep” soundings.

Geotechnical Borings and Standard Penetration Tests (SPT)

Eight geotechnical borings and SPT soundings were conducted at strategic locations across the site. Similar to above, the refraction tomograms and CPT results were used to select these locations. All of the borings included drilling and recovery of rock cores through a minimum of 3 m of material, and in one core, through 11 m of material. While space limitations do not allow presentation of these detailed boring log results herein, the following information is provided:

- Three of the eight borings were located along line A at the following stations: 19.8, 35.6, and 65.5 m. These borings coincided with CPT tests at 19.8 and 65.5, while the boring at 35.6 m was slightly to the left of the CPT sounding at 39.6 m.
- At station 19.8 m, the boring was advanced through predominantly sand overburden soil having SPT N-values less than 10 to a depth of 9.0 m. Below 9.0 m, coring was conducted to a depth of 12.5 m, and the material was reported to be tan limestone with fossils throughout. The recovery of this material was 100% throughout, and the rock quality designation (RQD) was reported as 100, except for the first 0.5 m which was broken at the top (RQD approximately 85).
- At station 35.6 m, the boring was advanced through sandy clay and sand overburden soil having SPT N-values between 7 and 10 to a depth of 2.3 m. Below 2.3 m, coring was conducted to a depth of 11.0 m, and the material was reported to be predominantly light tan to white limestone with fossils throughout.
- At station 65.5 m, the boring was advanced through sand overburden soil to a depth of only 0.3 m. Below 0.3 m, coring was conducted to a depth of 9.4 m, and the material was reported to be predominantly light tan to white limestone with fossils throughout. The recovery of this material varied between 80-100%, with approximately 60% of the run reported at the 100% recovery level. The boring notes report that several zones appeared to be weak and broken, and the RQDs varied widely between 30 and 100. Nearly half the run indicated an RQD between 60 and 80, a short distance (10%) at RQD of 100, and the remaining 40% reported a RQD between 30 and 60.

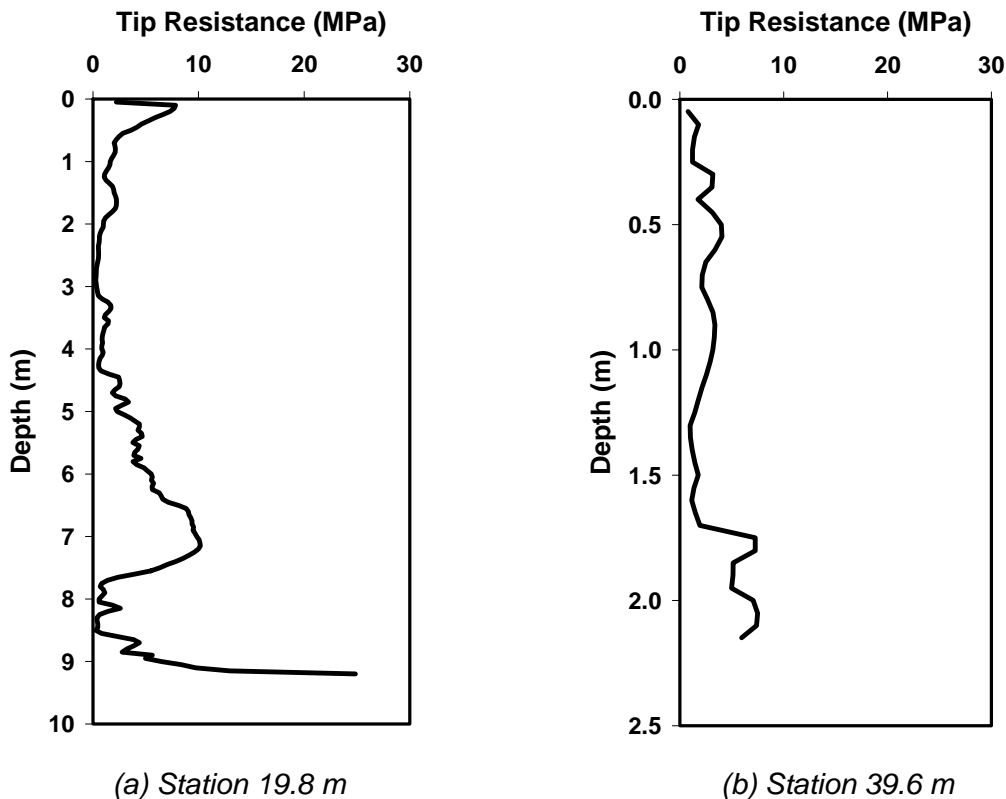
These results are compared with the refraction tomograms from figures 3b and 4b, and the CPT results from figure 5 as follows:

- The CPT and boring information at stations 19.8 and 65.5 m appear to be in good agreement. At 19.8, CPT testing was terminated upon approaching a limiting large value at a depth of 9.2 m, while boring information reported the overburden soil/rock interface at a depth of 9.0 m. Similarly, at 65.5, CPT testing was terminated at a depth less than 0.5 m, while the top of rock was reported at 0.3 m.
- The undulating, valley/bowl to block/pinnacle features noted along the P-wave velocity tomograms appear to be the result of lateral variation in the overburden soil/rock interface along the length of the refraction line. At 19.8, a valley/bowl feature appears, and the top of rock is found at 9.0 m, while at 65.5, a block/pinnacle feature appears, and the top of rock is found at 0.3 m.

- While the undulating features in the velocity tomograms are generally indicative of the soil/rock interface, the top of rock does not appear along a constant contour of P-wave velocity. Within a valley (station 19.8), the top of rock is found at approximately 2000 m/s, while at the top of a block (station 65.5), the top of rock is found at a velocity of approximately 500 m/s. However, the rock under station 19.8 m was reported competent and intact, with 100% recovery and RQD of 100 throughout all but a short length at top of core run, while the rock under station 65.5 m was reported to be of lower quality. Velocity differences between these two materials should be expected.
- Finally, it is very interesting to note that the CPT will penetrate a particulate, sand material of much higher velocity (station 19.8), than it will a rock of lower velocity (station 65.5). Velocity is related to the small-strain modulus of the material, while CPT tip resistance is related to bearing capacity or strength of the material. Even though the rock at station 65.5 has a relatively low velocity as measured through a large volume of material, the local strength beneath the cone tip is still large. A large, broken mass of this material under low confinement near the ground surface has low velocity. However, the local, broken pieces are still an intact, cemented material, and highly resistant to local CPT penetration. Alternatively, the particulate, sand material under large confinement at 9 m is considerably stiffer, yet will undergo local shear failure under CPT penetration. Thus, these results reinforce the premise that good site characterization practice should include measurement of multiple parameters to fully understand expected behavior.

Sinkhole Observations

As noted above, the seismic refraction testing was conducted at the site during summer 2005, followed by the CPT soundings in early November 2005, and finally the geotechnical borings in December 2005. Following a period of heavy rain and storm water runoff in February 2006, two sinkholes formed in the detention pond directly over the A line. The first sinkhole formed at approximately station 19.5 m, and the second at station 52.1 m. It is very interesting to note that these two locations appear as valley/bowl features in the P-wave velocity tomograms, and the feature at station 19.5 m was also well



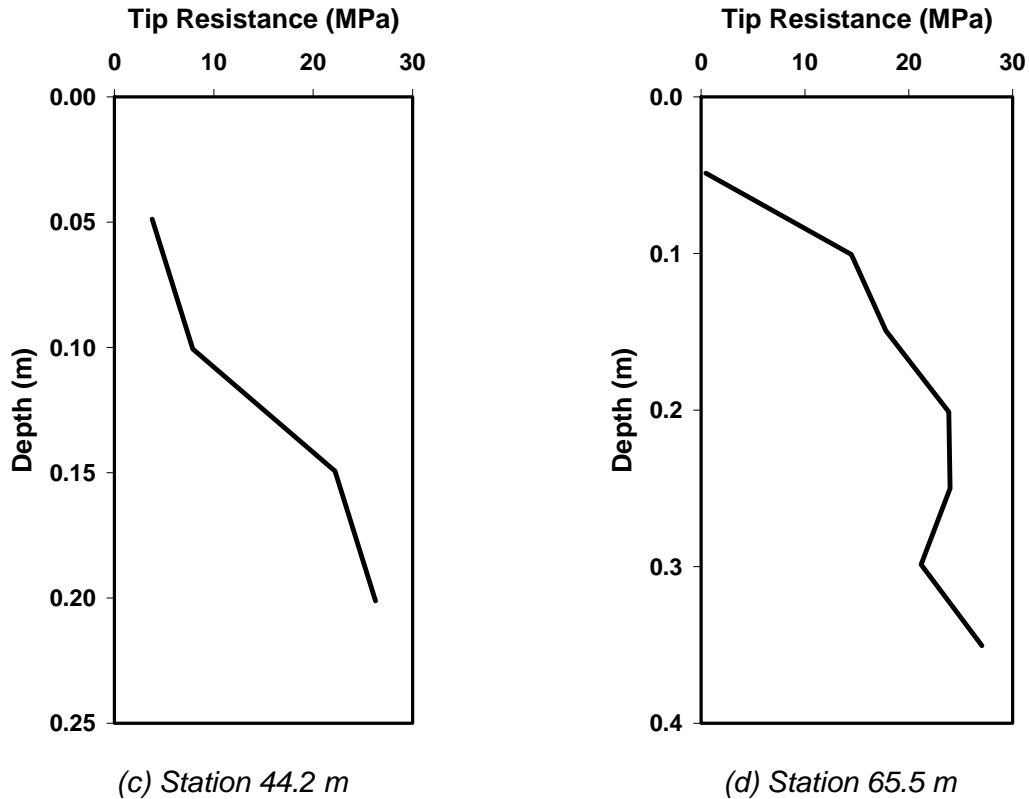


Figure 5. Cone Penetration Tip Resistances, Line A

identified by CPT and geotechnical boring results. It seems logical that sinkholes would be much more likely to form in such locations, rather than at the top of a block/pinnacle feature. Thus, it appears that seismic refraction tomography has potential in identifying high-risk areas for sinkhole development.

CONCLUSIONS

Karstic limestone is characterized by a typically undulating bedrock surface and the presence of numerous springs, cavities, and caves. Analysis of a seismic refraction study at the shared University of North Florida and University of Florida karstic limestone geophysical/ground proving test site in central Florida demonstrated that the Seisimager refraction tomography software system is able to reveal the typical undulating bedrock surface. However, compression wave velocities at the top of the bedrock within limestone valleys were significantly higher than the compression wave velocities at the top of blocks and pinnacles. Ground proving via cone penetration tests and geotechnical borings appears to corroborate this finding, and demonstrates the importance of measuring multiple material parameters during site characterization activities in complex terrane. Finally, two sinkholes formed in the detention pond directly over two valley/bowl features after refraction testing was completed, demonstrating that refraction tomography has potential in identifying areas at risk for sinkhole development.

ACKNOWLEDGEMENTS

This work was supported by the Florida Department of Transportation, District 2.

REFERENCES

- Campbell, K. M., and T. M. Scott, 1991, Radon potential study, Alachua County, Florida: Near-surface stratigraphy and results of drilling: Florida Geological Survey Open File Report Number 41.
- Carpenter, P. J., I. C. Higuera-Diaz, M. D. Thompson, S. Atre, and W. Mandell, 2003, Accuracy of seismic refraction tomography codes at karst sites: Geophysical Site Characterization: Seeing Beneath the Surface: Proceedings of a Symposium on the Application of Geophysics to Engineering and Environmental Problems, 832-840.
- Cramer, B. J., and D. R. Hiltunen, 2004, Investigation of bridge foundation sites in karst terrane via seismic refraction tomography: 83rd Annual Meeting Compendium of Papers CD-ROM, Transportation Research Board.
- Hayashi, K., and T. Takahashi, 2001, High resolution seismic refraction method using surface and borehole data for site characterization of rocks: International Journal of Rock Mechanics and Mining Sciences, **38**, 807-813.
- Hiltunen, D. R., and B. J. Cramer, 2006, Geophysical characterization of bridge foundation sites in karst terrane: 85th Annual Meeting Compendium of Papers CD-ROM, Transportation Research Board.
- Moser, T. J., 1991, Shortest path calculation of seismic rays: Geophysics, **56**, 59-67.
- Randazzo, A. F., 1997, The sedimentary platform of Florida: Mesozoic to Cenozoic, *in* A. F. Randazzo and D. S. Jones, eds., The geology of Florida: University of Florida Press.
- Scott, T. M., 2001, Text to accompany the geologic map of Florida: Florida Geological Survey Open File Report Number 80.
- Sheehan, J., W. Doll, and W. Mandell, 2005, An evaluation of methods and available software for seismic refraction tomography analysis: Journal of Environmental and Engineering Geophysics, **10**, 21-34.
- Sowers, G., 1996, Building on sinkholes – design and construction of foundations in karst terrain, ASCE Press.